

Experimental report

28/06/2022

Proposal: 7-01-541

Council: 10/2020

Title: Lattice dynamics in liquid-like thermoelectric material Ag₈GeSe₆

Research area: Materials

This proposal is a new proposal

Main proposer: Xingchen SHEN

Experimental team: Bjorn FAK
Xingchen SHEN

Local contacts: Bjorn FAK
Michael Marek KOZA

Samples: Ag₈GeSe₆

Instrument	Requested days	Allocated days	From	To
PANTHER	6	2	12/03/2021 30/06/2021	13/03/2021 01/07/2021

Abstract:

In thermoelectric (TE) materials research, a low lattice thermal conductivity is indispensable for high material performance. To this end, the liquid-like materials hold great promise. In this project we focus on Argyrodites with the composition Ag₈GeSe₆, a family of liquid-like TE materials. Our preliminary study [5] showed that the lattice thermal conductivities are below the amorphous limit despite the well-documented crystallinity; particularly, an unusual low temperature peak of lattice thermal conductivity is observed at $T \sim 7$ K, which might be attributed to strong anharmonic interactions between the heat carrying long wavelength acoustic phonons and the low-lying optical modes. Therefore, we propose to investigate the phonon density-of-states via inelastic neutron scattering in order to derive a coherent multi-scale understanding of lattice dynamics and heat conduction, with the emphases on the phonon mean free path in spatial domain and the phonon life time in temporal domain. The results emanated from this project will not only enrich our knowledge on heat conduction at large but also facilitate developing novel TE materials beyond the class of semiconductors.

Experimental report

Lattice dynamics in liquid-like thermoelectric material Ag_8GeSe_6

Abstract:

In addition to conventional thermoelectric study that is on electronic conductors (semiconductors and semimetals), many special interests are currently focused on liquid-like materials, e.g., $(\text{Cu}, \text{Ag})_2\text{Se}^{[1]}$, $(\text{Ag}, \text{Cu})\text{CrSe}_2^{[2-3]}$, in which the complex interplay among mobile ions and that between mobile ions and the rest of crystal lattice leads to intrinsically low κ_L in superionic phases. Other than the well-known prototypical $(\text{Cu}, \text{Ag})_2\text{Se}$ and $(\text{Ag}, \text{Cu})\text{CrSe}_2$, Argyrodites with a general chemical formula A_8BX_6 ($\text{A} = \text{Cu}, \text{Ag}$; $\text{B} = \text{Si}, \text{Ge}, \text{Sn}$; and $\text{X} = \text{S}, \text{Se}, \text{and Te}$) are interesting in their own right and undergo multiple phase transitions towards a face-centered cubic structure, indicative of closely competing thermodynamic states. Ag_8GeSe_6 exhibits the weak temperature dependence and low magnitude κ_L along with decent electrical performances at high-temperature cubic superionic phase^[4] in the virtue of the partially occupied mobile Ag-sublattice interpenetrating a rigid network of GeX_4 tetrahedra. However, the fundamental understanding of the interesting thermal transport in terms of temporal-spatial lattice dynamics and atomic diffusion in the superionic phase of Argyrodites remains unexplored. Herein, for the sake of further obtaining more insights into the thermal transport properties in terms of lattice and diffusive dynamics aspects, we perform the inelastic neutron scattering (INS) and quasi-elastic neutron scattering (QENS) on the Ag_8GeSe_6 power sample. Our recent high-temperature synchrotron x-ray diffraction suggests Ag_8GeSe_6 enters into the cubic phase ($F\bar{4}3m$) above 350 K. Particularly, Ag atoms undergo a superionic phase transition from static order to dynamic disorder state, accompanied by the jump-like Ag diffusion in the unoccupied lattice sites when it fully enters into the cubic phase.

In our experiments, we collected the low-temperature INS data from 2-200 K by using two incident energy $E_i=30.05$ and 50.29 meV in both energy loss and gain modes. In principle, the energy resolution is around 5-6% of the incident energy on the Panther spectrometer. Our INS measurements with relatively low $E_i=30.05$ meV enable us with high energy resolution for probing the low energy peaks, while the high $E_i=50.29$ meV assures us to obtain the whole phonon spectrum up to 40 meV. The corresponding high-temperature INS measurements with low $E_i=12.61$ meV provide a high energy resolution for obviously identifying and analyzing Ag diffusive dynamics. We use the Mantid package to process and analyze data^[5], and then subtract the background of the empty aluminum sample holder with the same E_i at different temperatures from the raw collected data. As depicted in the 2D-contour plotting in [Fig. 1(a-f)], we observe the ultralow-lying optical phonon mode with ~ 2 meV at 2 K and the intensity of the low-lying phonon modes below 5 meV is significantly increased from 2 to 200 K.

Experimental 2D-contour plotting of INS at 300-700 K are plotted in [Fig. 2(a-e)], respectively. In our high-temperature INS experiments from 300-700 K ($E_i=12.61$ meV) across $T_c \sim 350$ K, we observe a soft phonon (at $Q \sim 2.88 \text{ \AA}^{-1}$) as drawn in [Fig.2(a-b)] and a notably increased QENS signal (at $Q < 1.5 \text{ \AA}^{-1}$, e.g., $Q=1.4 \text{ \AA}^{-1}$, as shown in [Fig. 2(b-e)]. We further extract the $S(Q, E)$ with $E_i=12.61$ meV at $Q \sim 2.88 \text{ \AA}^{-1}$ from 2-400 K as presented in [Fig. 3(a)] (e.g., 300, 334, 355, and 400 K). The visible low energy modes with ~ 2 meV at 300 K gradually soften approaching T_c and finally merge with the elastic line after entering the superionic cubic phase, signifying the emergence of the QENS signal. As shown in [Fig. 3(b-d)], we fit the raw data of $S(Q, E)$ using a damped harmonic oscillator (DHO)/over-damped oscillator (ODHO) function^[6] which is convoluted with ~ 0.6 meV energy resolution, in combination with a Gaussian function and a flat background. The corresponding derived phonon energy as depicted in [Fig. 3(e)], displays a finite value below 350 K and then becomes an infinite zero value above 350 K, manifesting the occurrence of full phonon softening approaching the superionic phase and the coexistence of maintained full phonon softening and QENS signal above the superionic phase.

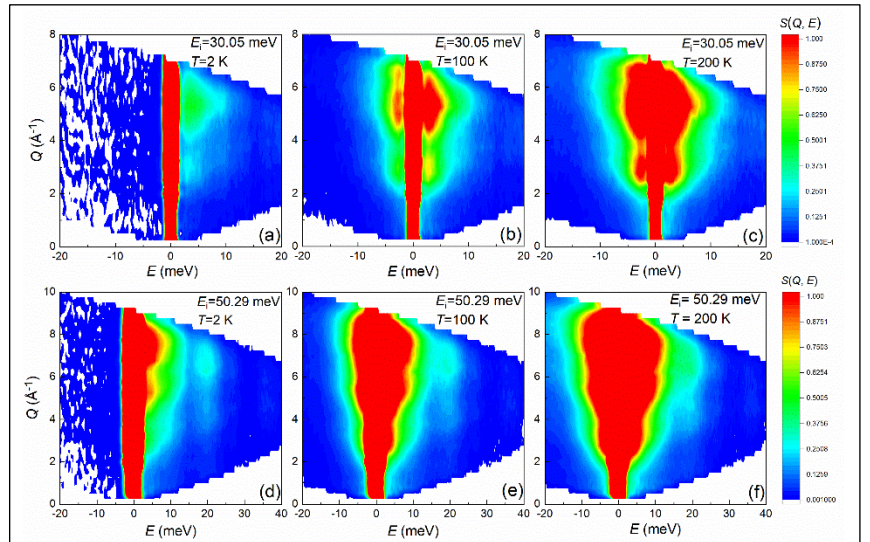


Fig. 1(a-f) Experimental $S(Q, E)$ data with $E_i=30.05$ meV from 2-200 K. (d-e) Experimental $S(Q, E)$ data with $E_i=50.29$ meV from 2-200 K.

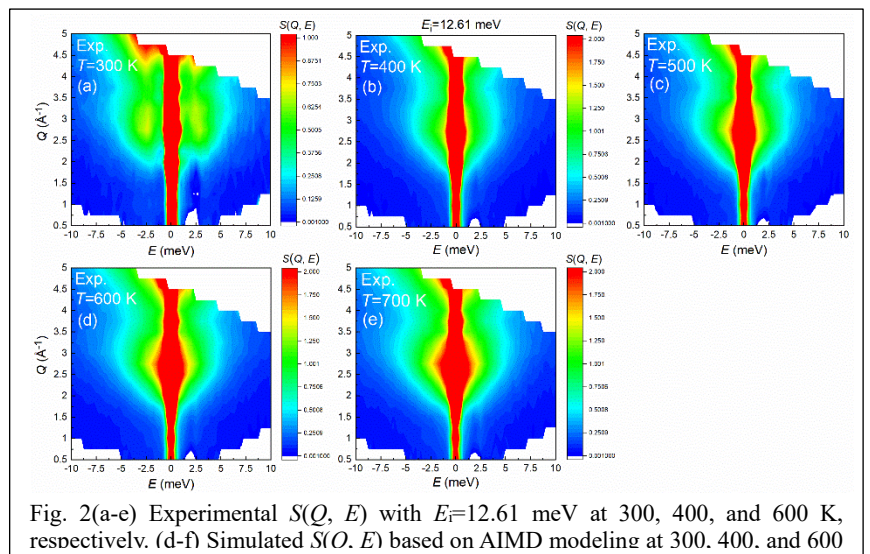


Fig. 2(a-e) Experimental $S(Q, E)$ with $E_i=12.61$ meV at 300, 400, and 600 K, respectively. (d-f) Simulated $S(Q, E)$ based on AIMD modeling at 300, 400, and 600 K, respectively.

As shown in [Fig. 3(b-d)], we fit the raw data of $S(Q, E)$ using a damped harmonic oscillator (DHO)/over-damped oscillator (ODHO) function^[6] which is convoluted with ~ 0.6 meV energy resolution, in combination with a Gaussian function and a flat background. The corresponding derived phonon energy as depicted in [Fig. 3(e)], displays a finite value below 350 K and then becomes an infinite zero value above 350 K, manifesting the occurrence of full phonon softening approaching the superionic phase and the coexistence of maintained full phonon softening and QENS signal above the superionic phase.

To accurately probe the Ag diffusive behavior from the QENS signal, we extract and analyze the QENS signals over the Q range of $[0.6, 1.4 \text{ \AA}^{-1}]$ due to the considerable contaminated low-lying phonon modes at a higher Q regime (e.g., $Q \sim 2.88 \text{ \AA}^{-1}$), which cannot be distinguishable from the contribution component of the experimental QENS signal. As presented in [Fig. 4(a-b)], e.g., at 373 and 700 K, the fitting of $S(Q, E)$ with a delta function (the measured data at 300 K), a Lorentzian function as well as a flat background, yields the Q -dependent full width half maximum (Γ , FWHM). Upon rising temperatures, the FWHM curves are slightly increasing, indicative of a shorter diffusion timescale corresponding to a faster Ag diffusion process at elevated temperatures. In order to quantitatively obtain the diffusive characteristics in terms of time-domain and length-domain, we further utilize the standard jump-diffusion Chudley-Elliots(CE) model^[7] to fit the experimental FWHM from 500-700 K (plotted as the colored solid lines in [Fig. 4(c-e)]), resulting in the T -dependent mean jump length and average residence time. Under the assumptions of the fixed jump length and Q -dependent FWHM of the expected atomic diffusion dynamics, the CE model can be formularized in **equation (1)**:

$$\Gamma(Q) = \frac{2\hbar}{\tau} \left(1 - \frac{\sin(Qd)}{Qd}\right)$$

Where τ and d are the average residence time and mean jump length at a specific momentum transfer Q . Further, the diffusion coefficient D are calculated from **equation (2)**:

$$D = \frac{d^2}{6\tau}$$

In combination with the surprisingly short residence time ~ 0.6 ps arising from its experimental broadening FWHM, we obtain the relatively high diffusion coefficients with the magnitude of $10^{-4} \text{ cm}^2 \text{ s}^{-1}$ in our QENS experiments, indicating the ultrafast diffusive dynamics in the superionic phase of Ag_8GeSe_6 .

In summary, we implement the neutron scattering on powder Ag_8GeSe_6 sample over a wide temperature regime. Our low-temperature INS experiments illustrate the low-lying optical phonon modes of the ground state which are responsible for the intrinsic anharmonicity and unusual low-temperature peak for κ_L observed at $T \sim 7$ K. Furthermore, our T -dependent INS measurements and simulated neutron spectroscopy observe the suppressed low-lying phonon modes and then gradually soften at T_c , finally evolve into the elastic line to form QENS signal. The INS results discriminate the diffusive Ag atoms resulting in the presence of the full phonon softening at T_c , and then the concurrently preserved full phonon softening and QENS signal above T_c . Based on the CE model, analysis of the experimental QENS of $S(Q, E)$ imply the ultrafast Ag diffusion with a short residence time of ~ 0.6 -1.0 ps and a diffusive length of $\sim 3 \text{ \AA}$, yielding a large diffusive coefficients magnitude of $\sim 1\text{e-}4 \text{ cm}^2 \text{ s}^{-1}$. Compared to the phonon lifetime, the diffusive relaxation time is relatively slow to effectively scatter the transport phonon.

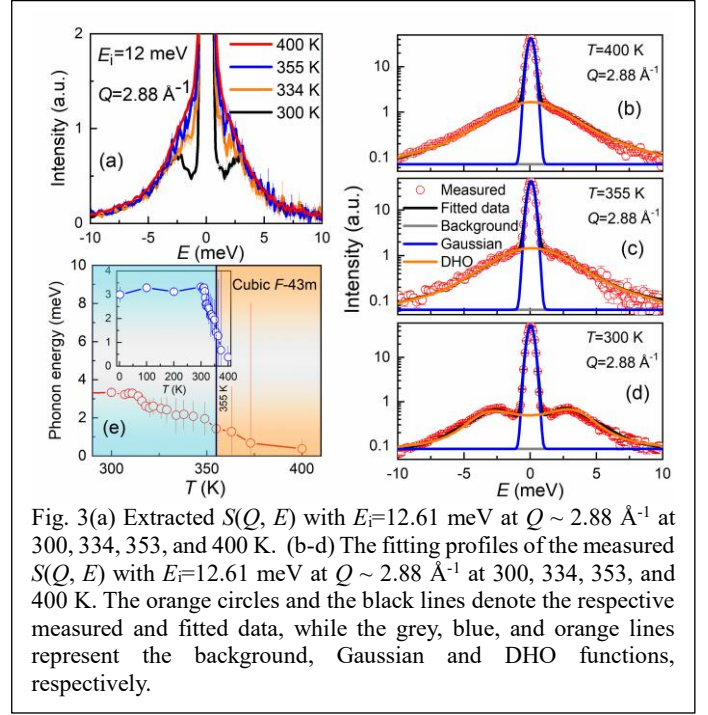


Fig. 3(a) Extracted $S(Q, E)$ with $E_i=12.61$ meV at $Q \sim 2.88 \text{ \AA}^{-1}$ at 300, 334, 353, and 400 K. (b-d) The fitting profiles of the measured $S(Q, E)$ with $E_i=12.61$ meV at $Q \sim 2.88 \text{ \AA}^{-1}$ at 300, 334, 353, and 400 K. The orange circles and the black lines denote the respective measured and fitted data, while the grey, blue, and orange lines represent the background, Gaussian and DHO functions, respectively.

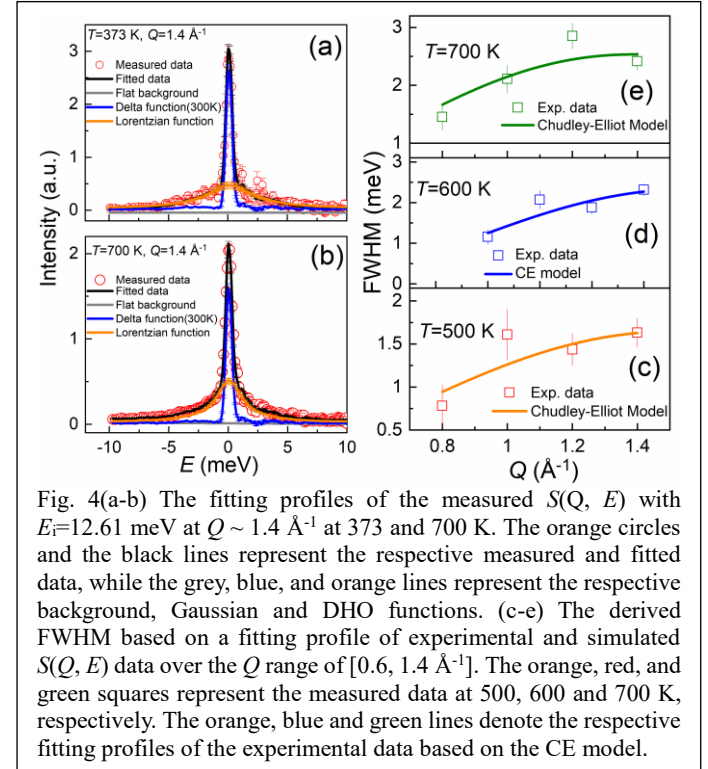


Fig. 4(a-b) The fitting profiles of the measured $S(Q, E)$ with $E_i=12.61$ meV at $Q \sim 1.4 \text{ \AA}^{-1}$ at 373 and 700 K. The orange circles and the black lines represent the respective measured and fitted data, while the grey, blue, and orange lines represent the respective background, Gaussian and DHO functions. (c-e) The derived FWHM based on a fitting profile of experimental and simulated $S(Q, E)$ data over the Q range of $[0.6, 1.4 \text{ \AA}^{-1}]$. The orange, red, and green squares represent the measured data at 500, 600 and 700 K, respectively. The orange, blue and green lines denote the respective fitting profiles of the experimental data based on the CE model.

Reference

1. Liu H. L. *et al. Nat. Mater.* 2012, **11** (5), 422-425.
2. Niedziela, J. L., *et al. Nature Physics* 2019, 15.1: 73-78.
3. Ding, J. X., *et al. Proceedings of the National Academy of Sciences* 2020, 117.8: 3930-3937.
4. Anek C. *et al Jpn. J. Appl. Phys.* 2009, **48**, 011603.
5. Arnold O, *et al. Detectors and Associated Equipment* 764, 156-166 (2014).
6. Fåk B, *et al. Phonon line shapes and excitation energies.* 1107-1108 (1997).
7. Chudley CT, *et al. Proceedings of the Physical Society* **77**, 353-361 (1961)